Punjab University Journal of Mathematics (2025), 57(06), 670- 686
https://doi.org/10.52280/pujm.2025.57(06)04

An optimisation over the Möbius group for an optimal solution in image registration

Received
13 March, 2025

Revised
11 November, 2025

Accepted
17 November, 2025

Published Online
28 November, 2025

*M. Y. Tufail
Department of Mathematics,
NED University of Engineering & Technology, Karachi,
Pakistan

S. Gul
Department of Mathematics,
NED University of Engineering & Technology, Karachi,
Pakistan

Abstract. Image registration, the process of aligning two images to ensure their appearances closely match, is a field profoundly influenced by the pioneering contributions of D'Arcy Wentworth Thompson. In his influential work *On Growth and Form*, Thompson introduced the concept of image transformation across species, emphasising the idea that deformations between closely related species should exhibit simplicity. Specifically, Thompson explored isogonal transformations—now known as conformal transformations—suggesting that such deformations could be described by finite dimensional groups. While the full set of diffeomorphisms or the conformal group are too complex to be considered simple (as they are infinite), the eight-dimensional Möbius group, a subgroup of the conformal group, provides a more manageable framework. The Möbius group comprises four fundamental transformations: scaling, rotation, translation, and inversion, offering a balance between simplicity and mathematical expressiveness.

In this study, we propose a novel approach to image registration using Möbius diffeomorphisms. Additionally, an innovative method for selecting the initial guess, a critical component in the optimisation process, particularly within the gradient descent framework, has been introduced. Through a series of numerical examples, we demonstrate the effectiveness of this approach in achieving precise and efficient Möbius-based image registration. Our results highlight the potential of Möbius transformations as a robust tool for image alignment, bridging historical theoretical insights with contemporary computational methodologies. This work not only advances the field of image registration but also underscores the enduring relevance of Thompson's foundational ideas in modern scientific research.

*Corresponding Author: tufail@neduet.edu.pk

AMS (MOS) Subject Classification Codes: 68U10; 78M50; 37C05; 51B10

Key Words: Möbius transformations, Optimisation, Conformal transformations, Image registration.

1. INTRODUCTION

Image registration, the process of aligning two images to achieve similarity in their appearances, is a widely studied technique across diverse fields such as computer vision [13, 37, 53], remote sensing [1, 12, 49], morphophonemics [6, 8, 14, 32, 33, 42, 46], medical imaging [2, 11, 21, 22, 23, 25, 26, 29, 31, 35, 41, 44, 47], and shape analysis [45, 51, 52], among others. The foundations of image registration can be traced back to the pioneering investigation of Thompson, whose groundbreaking 1917 book 'On Growth and Form' [48] introduced the concept of image transformation across species. Thompson's ideas have profoundly influenced the study of diffeomorphic deformations in images, particularly in medical image registration. Despite significant advancements since 1917, one of the most notable developments has been the pursuit of diffeomorphisms between images, exemplified by the 'Large Deformation Diffeomorphic Metric Mapping (LDDMM)' framework [4,10,17,19,27].

In 1992, Brown [9] provided a comprehensive review of image registration, outlining its fundamental steps, many of which remain relevant today. Brown identified four core components: (i) a feature space (containing image information), (ii) a search space (encompassing possible transformations), (iii) a search strategy (for selecting optimal transformations), and (iv) a similarity metric (to quantify discrepancies between images). While Brown's work focused on finite-dimensional transformations—such as affine, perspective, and polynomial transformations—the field has since expanded to include more sophisticated methods, including diffeomorphic image registration. Diffeomorphisms, which are smooth and invertible transformations, have become central to this area of research [51, 52, 54].

Thompson's work employed hand-drawn illustrations of animal forms with superimposed grids, demonstrating smooth deformations between species. These transformations, which preserve smoothness, are now recognized as foundational to diffeomorphic image registration. Thompson also explored isogonal transformations, now referred to as conformal transformations, which preserve angles. His observations on conformal relationships between species were further investigated by Petukhov [39], who applied Thompson's grid method and computed the cross-ratio—an invariant of the Möbius group—to assess whether point sets could be related by Möbius transformations. Petukhov's findings suggested that Möbius transformations may play a role in certain instances of growth and evolution.

Inspired by Thompson's examples [48] and Petukhov's work [39], the applicability of Möbius transformations [3, 30, 36, 40] is investigated using image registration techniques rather than point-based invariants. Specifically, image registration is performed by minimizing the SSD [50] between pixel intensities in order to evaluate the extent to which image relationships align with conformal transformations.

Furthermore, a novel method for selecting initial guesses in image registration (illustrated in Examples 2 and 3), a critical factor in optimisation, is introduced. All registration processes involving Möbius diffeomorphisms are conducted on two-dimensional grayscale images [51, 52]. This approach allows us to rigorously assess the role of Möbius transformations in image registration and their potential applications in conformal mapping.

2. MÖBIUS GROUP

In this section we first discuss the Möbius group, a well established sub-group of the group of conformal transformations (typically called diffeomorphisms in image registration), and then the registration over the Möbius group would be presented. There is natural isomorphism between the Euclidean plane $\mathbb{R}^2$ and its contemporary complex plane $\mathbb{C}$, i.e., $\mathbb{R}^2 \cong \mathbb{C}$. This fact allow us to consider image domain Ω as a domain of complex plane $\mathbb{C}$. In fact, Möbius transformations, which are a type of diffeomorphism, are most effectively understood when considered as mappings of the *extended complex plane*,

denoted as $\hat{\mathbb{C}} = \mathbb{C} \cup \{\tilde{\infty}\}$, to itself. In this context, $\tilde{\infty}$ represents *complex infinity*, an extension of the complex plane that allows for a more comprehensive treatment of the transformation's behavior, particularly at the limits of the complex plane. The extended

complex plane, $\hat{\mathbb{C}}$, is also known as the *Riemann sphere*, a concept named after the German mathematician Bernhard Riemann. The Riemann sphere is a geometric representation of the complex plane that includes the point at infinity, transforming the complex plane into a sphere-like structure where transformations can be interpreted in a more elegant and unified way. This viewpoint is essential in various areas of mathematics, such as complex analysis and geometry, and helps to reveal the deeper symmetries and properties of Möbius transformations. As such, Möbius transformations are typically seen as bijective conformal mappings of the Riemann sphere onto itself, preserving both the structure of angles and the shape of objects, which makes them particularly useful in the study of conformal geometry and hyperbolic spaces [5, 20,38].
A Möbius transformation is defined as:

$$\varphi(z) : \hat{\mathbb{C}} \to \hat{\mathbb{C}} = \frac{pz+q}{rz+s}; p, q, r, s \in \hat{\mathbb{C}} \& ps - qr \neq 0. \tag{2. 1}$$

It is important to pay attention to the fact that when $r = 0$ in Eq. (2. 1), the transformation simplifies to a rigid transformation [50], where the first term, $\frac{p}{s}z$, causes the rotation along with scaling, and the second term, $\frac{q}{s}$, is responsible for translation. This demonstration highlights the fact that rigid group is inside the Möbius group, i.e., a subgroup. A Möbius transformation can be constructed by composing four fundamental transformations: rotation, scaling inversion, and translation [16]. In Proposition 2.1, the derivation of Eq. (2. 1) by combining above mentioned transformations is presented.

Proposition 2.1. *A Möbius transformation is the composition of four simple transformations that are scaling, rotation, translation and inversion.*

Proof. For a complex number $z, \forall p, q, r, s \in \hat{\mathbb{C}}$, the following four transformations are employed: translation, inversion, scaling and translation, and translation, respectively.

$$\psi_1(z) = z + \frac{s}{r}. \tag{2. 2}$$

$$\psi_1(z) = \frac{1}{z}. \tag{2. 3}$$

$$\psi_3(z) = \frac{-ps + qr}{r^2} z. \tag{2. 4}$$

$$\psi_4(z) = z + \frac{p}{r}.$$

Now, composition yields:

$$\begin{aligned}
\psi_4 \circ \psi_3 \circ \psi_2 \circ \psi_1 &= \psi_4 \circ \psi_3 \circ \psi_2(z + \frac{s}{r}), \quad \text{From 2. 2} \\
&= \psi_4 \circ \psi_3(\frac{1}{z + s/r}), \quad \text{From 2. 3} \\
&= \psi_4(\frac{-ps + qr}{r(rz + s)}), \quad \text{From 2. 4} \\
&= \frac{pz + q}{rz + s} \\
&= \varphi(z).
\end{aligned}$$

□

The set of Möbius transformations (or diffeomorphisms) form a group under composition. Illustration is given below:

- **Composition of two Möbius transformations**

  The composition of two Möbius transformations yields another Möbius transformation.

  Suppose $\varphi_1(z) = \frac{pz+q}{rz+s}$ and $\varphi_2(z) = \frac{p'z+q'}{r'z+s'}$.

$$\begin{aligned}
(\varphi_1 \circ \varphi_2)(z) &= \varphi_1(\varphi_2(z)) \\
&= \varphi_1(\frac{p'z + q'}{r'z + s'}) \\
&= \frac{p(\frac{p'z+q'}{r'z+s'}) + q}{r(\frac{p'z+q'}{r'z+s'}) + s} \\
&= \frac{(pp' + qr')z + (pq' + qs')}{(rp' + sr')z + rq' + ss'} \\
&= \frac{Pz + Q}{Rz + S}
\end{aligned}$$

  Where, $P = pp' + qr', Q = pq' + qs', R = rp' + sr', S = rq' + ss'$. This property is often called the closure property in the 'Group Theory'.

- **Associativity**
  Using the concept of composition (as explained above), for any choice of p, q, r, s, one can easily derive the associativity of any three Möbius transformations $(\varphi_1, \varphi_2, \varphi_3)$. That is, $\varphi_1 \circ (\varphi_2 \circ \varphi_3) = (\varphi_1 \circ \varphi_2) \circ \varphi_3$.
- **Existence of the identity**
  This set includes an identity element, given by $id = \frac{1z+0}{0z+1}$. Using composition, it is straightforward to derive that $(\varphi_1 \circ id) = \varphi_1$.
- **Existence of inverse**
  As we know, the concept of image registration depends on the existence of inverse diffeomorphic function. Therefore, such existence for each element in the set of Möbius transformations is a crucial requirement. We now derive the inverse element as below:
  Suppose $\varphi^{-1}(z) = \frac{az+b}{cz+d}$ is the inverse of $\varphi = \frac{pz+q}{rz+s}$. The existence of $a, b.c.d$ will conform the existence of inverse.

$$\begin{aligned}(\varphi \circ \varphi^{-1})z = \varphi(\varphi^{-1})z = id(z)\\ \varphi(\frac{az+b}{cz+d}) = \frac{1z+0}{0z+1}.\end{aligned} \tag{2. 5}$$

Eq. (2. 5) implies the following system of linear equations

$$\begin{aligned}pa + qc = 1\\ pb + qd = 0\\ ra + sc = 0\\ rb + sd = 1\end{aligned}$$

Consistent solution of above non-homogeneous system yeilds, $a = \frac{-s}{rq-sp}, b = \frac{q}{rq-sp}, c = \frac{r}{rq-sp}$ & $d = \frac{-p}{rq-sp}$. Plugin these values in φ^{-1} and few sreps of simplification will give:

$$\varphi^{-1}(z) = \frac{sz-q}{p-rz} \tag{2. 6}$$

Eq. (2. 6) can be recognized as a new Möbius diffeomorphisms in a Möbius group. Thus, the collection of Möbius transformations constitutes a group under composition. We now present an important proposition that require its existence as far as image registration is concerned.

Proposition 2.2. *If the composition of Möbius diffeomorphisms is defined within the domain $\Omega \subset \mathbb{R}^2$, the following equation holds:*
$(\Psi_1 \circ \Psi_2).(J(\boldsymbol{Y})) = \Psi_1.(\Psi_2.J(\boldsymbol{Y})), \forall \Psi_1, \Psi_2 \in Mob(\Omega, \mathbb{R}^2), \boldsymbol{Y} \in \Omega$
where '.' and $\circ$ respectively represent the action of Ψ on J and the composition, and $Mob(\Omega, \mathbb{R}^2)$ denotes the set of Möbius diffeomorphisms.

Proof. Suppose $\Psi_1, \Psi_2 \in Mob(\Omega, \mathbb{R}^2)$ in Ω such that their composition $\Psi_1 \circ \Psi_2$ is also a diffeomorphism in Ω, then

$$\begin{aligned}(\Psi_1 \circ \Psi_2).J(\mathbf{Y}) &= J((\Psi_1 \circ \Psi_2)^{-1}(\mathbf{Y})),\\ &= J((\Psi_2^{-1} \circ \Psi_1^{-1})(\mathbf{Y})),\\ &= J(\Psi_2^{-1}(\mathbf{Y}) \circ \Psi_1^{-1}(\mathbf{Y})),\\ &= J \circ \Psi_2^{-1}(\mathbf{Y}) \circ \Psi_1^{-1}(\mathbf{Y}),\\ &= (J \circ \Psi_2^{-1}(\mathbf{Y})) \circ \Psi_1^{-1}(\mathbf{Y}),\\ &= (\Psi_2.J(\mathbf{Y})) \circ \Psi_1^{-1}(\mathbf{Y}),\\ &= \Psi_1.(\Psi_2.J(\mathbf{Y})).\end{aligned}$$

□

Note 1. Although the four complex numbers (p, q, r, s) in Eq. (2. 1) may seem to represent 8 real parameters, the transformation with parameters $(\eta p, \eta q, \eta r, \eta s)$ is actually equivalent to the transformation with the original parameters (p, q, r, s) for any $\eta \in \mathbb{C}$. In other words, multiplying all the parameters by a complex factor η does not affect the transformation.
A common normalization choice for the parameters (p, q, r, s) is to impose the condition $ps - qr = 1$. This constraint simplifies the analysis by reducing the number of independent parameters (8 parameters to six parameters here).
In our study, the domain Ω is centered at the origin, and the singularity of the function $\varphi(z)$ occurs at $z = -s/r$. To ensure that this singularity lies outside the domain Ω, we choose to set $s = 1$, which leads us to the following parametrization for the transformation.

$$\varphi(z) = \frac{pz + q}{rz + 1}, \tag{2. 7}$$

where we require that $-1/r \notin \Omega$ to avoid singularities. We now formally define the image registration under Möbius diffeomorphisms.

Definition 1. *Suppose J_1, J_2 be two grayscale images. The difference between these images is quantified using the following error function, also known as the objective function:*

$$E(\Psi) = \int_\Omega \{(J_1 \circ \Psi^{-1})(\boldsymbol{Y}) - J_2(\boldsymbol{Y})\}^2 dx_1 dx_2, \boldsymbol{Y} = (y_1, y_2)^T \in \Omega \subset \mathbb{R}^2 \tag{2. 8}$$

Where Ψ denotes an element of the Möbius group, the phenomena of obtaining an optimal Ψ that minimizes Eq. (2. 8) is referred to as Möbius registration.

It is evident that Eq. (2. 8) represents the continuous version of the objective function. For numerical computation, we discretize this continuous version. Let us define the discrete domain $\mathbb{D}$, which serves as the domain for all the images presented in this paper. We suppose M, a positive integer, and $\mathbb{D} = \{([0, M - \beta]/(M - \beta) - 0.5) \times ([0, M - \beta]/(M - \beta) - 0.5); \beta = 1\}$ is a uniform square grid that contains $(M - 1)^2$ grid points, a simple example by setting $M = 100$ is

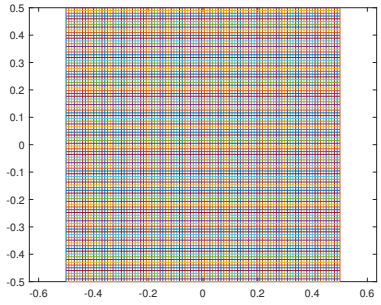

FIGURE 1. A square grid (our domain) with the range for data points is: $\{[-\alpha,\gamma]\times[-\alpha,\gamma];\alpha=\gamma=\frac{1}{2}\}$ with 100 grid points corresponding to each side, i.e., $M=100$.

shown in Fig. 1. We consider $M=100$ for all the numerical examples in this paper. The discrete form of objective function which is defined in Eq. 2. 8 is:

$$E(\Psi)=\sum_{i=1}^{M}\sum_{j=1}^{M}((J_1\circ\Psi^{-1})(Y_{ij})-J_2(Y_{ij}))^2. \tag{2. 9}$$

We would like to emphasize that the values of J_1 are specified at the uniform grid points, i.e., at Y_{ij}, rather than at $\Psi^{-1}(Y_{ij})$. Additionally, it should be clarified that the domain of $J_1\circ\Psi^{-1}$ is not Ω, but rather $\Psi(\Omega)$ at the continuous level. It is worth noting that for certain points, $J_1\circ\Psi^{-1}$ may extend outside of Ω during registration. Therefore, Ω is considered a restricted subset of $\mathbb{R}^2$. For computational purposes, we use the following values of $J_1\circ\Psi^{-1}(Y_{ij})$:

- If $\Psi^{-1}(Y_{ij})\in\Omega$, a bilinear interpolation using the MATLAB function `interp2` is applied, utilizing the values of J_1 at the four neighbouring corners of the corresponding quadrilateral.
- If $\Psi^{-1}(Y_{ij})\notin\Omega$, a constant white background (i.e., pixel value of 1) is used for all the examples.

Eq. (2. 9) presents the standard formulation of the least-squares optimisation function, applicable to any chosen group of planar transformation. This formulation represents a typical numerical optimisation problem, which falls under a broad and well-established field of study. Optimisation is a vast area of research with a wide array of algorithms tailored to different types of objective functions, each designed to address specific challenges in minimizing or maximizing a given function [28, 24]. While optimisation as a field is rich and diverse, the focus here is not to delve into its comprehensive theory, but rather to highlight a few simple and practical applications of these algorithms in the context of planar transformations.

2.3. **Image Registration.** We will start by exploring synthetic data sets, encompassing both smooth and non-smooth cases, where the relationship between the target and the source is governed by a well-defined Möbius transformation. Following this, we will shift our focus to non-synthetic data, where the connection between the images is not

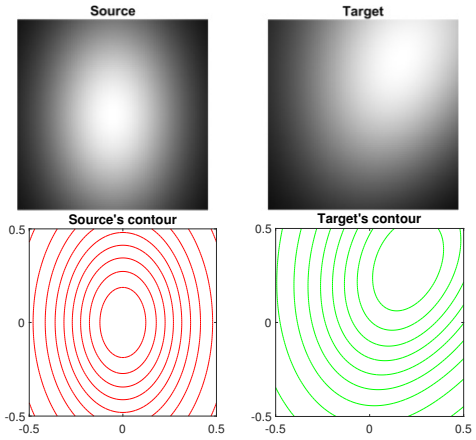

FIGURE 2. A collection of smooth images (Synthetic data). *Top:* The source data follows a Gaussian distribution. The target data is then generated by applying a Möbius transformation to the source data. *Bottom:* The contour plots of respective images, illustrating their respective shapes and relationships.

predefined. In all these scenarios, we will utilize a discrete domain, denoted as $\mathbb{D}$, which, as previously described, is defined for $M = 100$.

Example 1. In this first warm-up example, let us consider a synthetic dataset consisting of smooth images. These images are presented in Fig. 2. This particular case is slightly easier than the general problem of image registration because images are smooth and the target is known. The source image is the Gaussian ellipse (i.e., $e^{-7x^2-3y^2}$). The target is generated by applying a six-parametric Möbius transformation to the source image. The transformation is characterized by the coefficients $p = \sqrt{3/2}+\mathrm{i}(1/2)$, $q = 1/5-\mathrm{i}(3/10)$, and $r = 1/10 - \mathrm{i}(1/5)$.
To initiate the process, we use the identity transformation as the starting point, which corresponds to the values $p_{\text{ini}} = 1$, $q_{\text{ini}} = 0$, and $r_{\text{ini}} = 0$. The MATLAB optimisation function *lsqnonlin* [34] is employed to refine these initial estimates, and it returns the optimised values: $p_{\text{opt}} = \sqrt{3/2} + \mathrm{i}(1/2)$, $q_{\text{opt}} = 1/5 - \mathrm{i}(3/10)$, and $r_{\text{opt}} = 1/10 - \mathrm{i}(1/5)$.
The results of the image registration, as shown in Fig. 3, reveal an excellent alignment between the source and target images. This outcome demonstrates that the optimiser successfully converged to the optimal solution.

Example 2. This serves as a second example of synthetic data, though it differs from the previous one in that we are now working with a pair of non-smooth images. To generate the target image, a Möbius transformation with the parameters $p = \sqrt{3/2} + \mathrm{i}(1/2)$, $q = 1/5 - \mathrm{i}(3/10)$, and $r = 7/10 - \mathrm{i}(3/5)$ is applied. The resulting pair of images can be seen in Fig. 4.
We begin by setting the starting guess at the identity for the optimiser. Due to optimisation, the following optimised values are obtained: $p_{\text{opt}} = 1.01 - 0.00\mathrm{i}$, $q_{\text{opt}} = 0.002 - 0.002\mathrm{i}$,

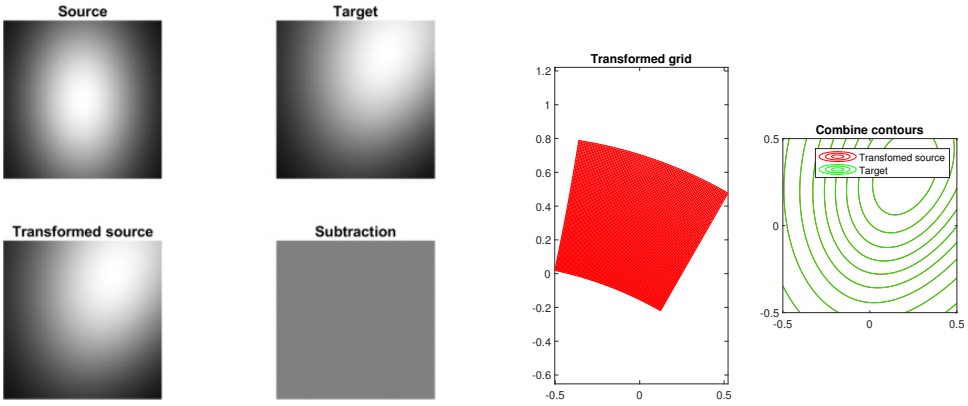

FIGURE 3. The outcomes obtained due to Möbius registration in Example 1, using the $lsqnonlin$ algorithm with the identity transformation as the initial guess, demonstrate a flawless alignment between the images. The registration process successfully minimized the discrepancy between the two datasets, resulting in an excellent match.

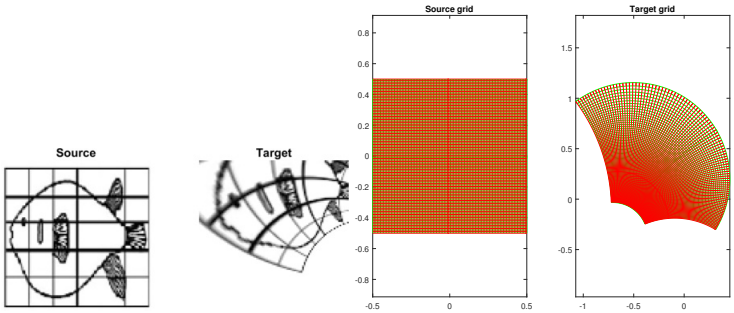

FIGURE 4. Set of synthetic non-smooth data.

and $r_{\text{opt}} = 0.0038 + 0.0072\text{i}$. These values are very close to the identity, leading us to suspect that a perfect registration may not be achieved. The outcome of this experiment, presented in Fig. 5, are poor. The possible explanation is that the optimiser got stuck at a local minimum and never came out from the valley.

A novel strategy for acquiring an initial approximation, known as labelled points (or landmarks) registration, is therefore proposed. This method draws inspiration from image registration using labelled points (see [27, 18, 7]), in which pairs of points $y_j \in \Omega$ and y'_j for the source and target are identified. The discrepancy function $\sum_j ||\varphi(y_j) - y'_j||^2$ is then minimized over $\varphi \in \text{Mob}(\Omega, \mathbb{R}^2)$. Since this objective function does not directly involve the images, the optimisation process is considerably easier. However, selecting the landmarks is a significant additional task. Automatic landmark selection remains a major

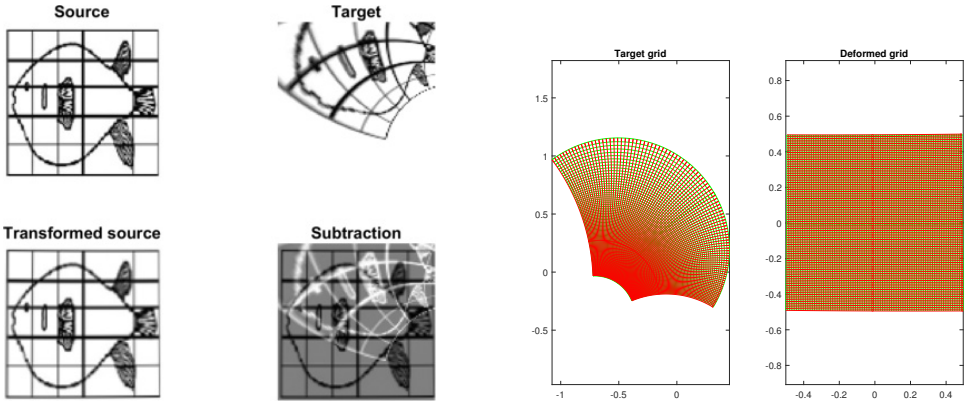

FIGURE 5. First attempt of image registration for Example 2. Results are poor.

research topic in the image processing community [15, 43]. Despite extensive work in this area, it is still a challenging problem, and in practice, landmarks are often chosen manually. In this approach, a marginally altered perspective is adopted. By virtue of the distinct property of the Möbius transformation, it is known that a mapping can always be chosen between three distinct points on the source and the target. This can be leveraged by restricting attention to three appropriate landmarks. Additionally, the desired Möbius transformation is obtained by solving a system of three linear equations.

Let y_j and y'_j $(j = 1, 2, 3)$ denote three isomorphic points over the respective grids (i.e., source and the target). The desired Möbius transformation that generates one one correspondence between y_j and y'_j satisfies the following system of equations:

$$\begin{aligned} y'_j =& \frac{py + q}{ry + 1}, \quad j = 1, 2, 3 \\ =& py_j + q - ry_j y'_j. \end{aligned} \tag{2. 10}$$

By solving these three linear equations, the parameters p, q, and r are obtained, which align the three selected labelled points (though not the images themselves). These variables are then used as the initial estimate for the optimisation process. In this example, the selected labelled points are illustrated in Fig. 6, and the optimisation results are $p_{opt} = \sqrt{3/2} + \mathrm{i}(1/2)$, $q_{opt} = 1/5 - \mathrm{i}(3/10)$, and $r_{opt} = 7/10 - \mathrm{i}(3/5)$. The outcomes of the optimisation are given in Fig. 7, where an excellent matching is achieved between the images.

Example 3. We now apply the landmark-based approach to generate an initial estimate for optimisation in a more intricate scenario. This example contains a pair of non-smooth images from Thompson's collection with no known Möbius transformation. The original images of Thompson's fish can be found in [48]. For this particular experiment, the images were scanned and the border of each image was outlined with a black marker. Undesired lines in the background grid for each image were removed digitally. The interior of the

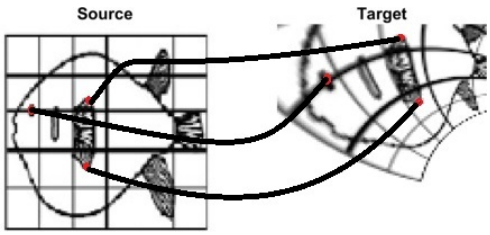

FIGURE 6. Selection of landmarks at corresponding positions in the source and target for Example 2.

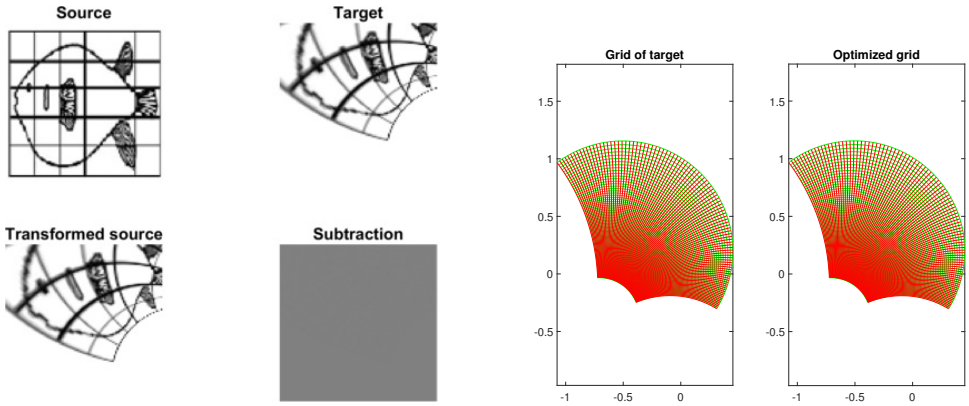

FIGURE 7. The refined attempt for the image registration using Möbius diffeomorphism for Example 2 are shown, where the initial guess is derived from landmark matching. This time, a perfect registration is achieved, demonstrating the effectiveness of using landmark-based initial guesses for the optimisation process.

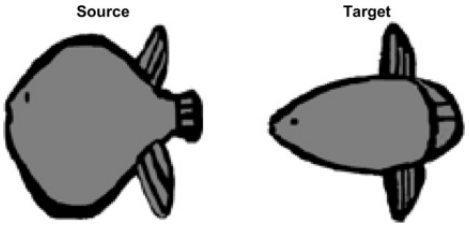

FIGURE 8. A cartoon rendition of Thompson's fish for for Example 3.

fish has been shaded grey—to facilitate the optimisation process—using Microsoft Paint as shown in Fig. 8. Subsequently, MATLAB's `imresize` routine is used for resizing each image upto 100×100 pixels.

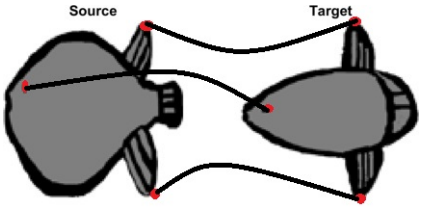

FIGURE 9. First set of landmarks for Example 3

Fig. 9 illustrates corresponding labelled points in both the images. The novel strategy of Example 2 produced the results of registration, between a pair of fish, that are presented in Fig. 10. As a result of this experiment, it is evident that the tail and fins are perfectly aligned, though the body shape does not exhibit the same level of alignment. The final step of the optimisation resulted in only a minor adjustment to the labelled points registration, which is evident in the slight misalignment of the eyes.

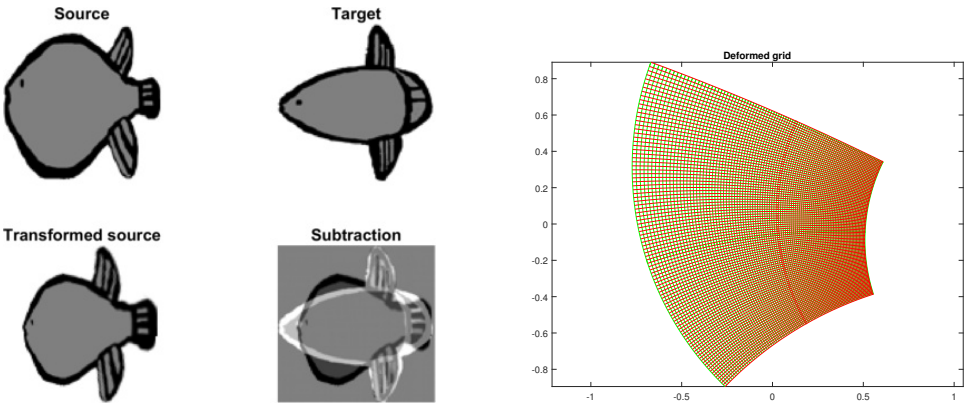

FIGURE 10. Image registration using Möbius group (due to first choice of landmarks) for Example 3.

We replicate this example with a different set of labelled points, as depicted in Fig. 11. The results are presented in Fig. 12. As before, the optimiser has made only a minor adjustment to the landmark alignment, and the body shapes remain poorly matched.

Let us explore an alternate option of registration by swapping the pair, i.e., source of the above registrations would be the target and vice versa (in the upcoming registrations) as depicted in Fig. 13. The labelled points are depicted in Fig. 14, and the results of the image registration are presented in Fig. 15.

Once again, the tail and fins are perfectly-aligned, but the whole shape remains less accurately registered. Nevertheless, the optimiser has made a significant adjustment to the labelled points matching, as evident in the positioning of the fish mouths. Notably, the conformal map obtained closely resembles to Thompson's grid [48].

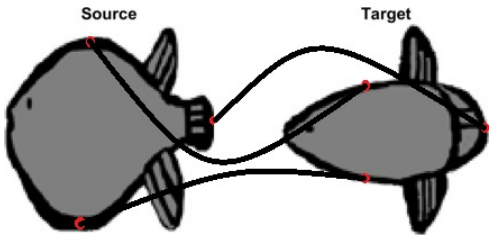

FIGURE 11. Second choice of landmarks are given for Example 3.

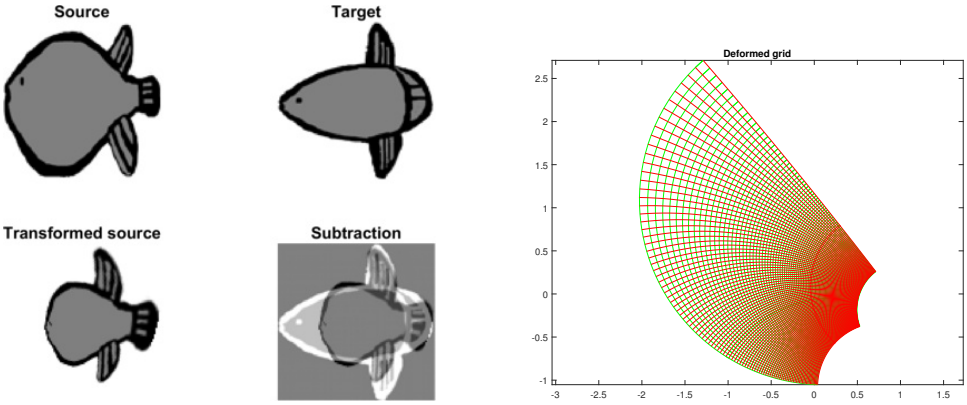

FIGURE 12. Möbius registration due to second choice of landmarks for Example 3.

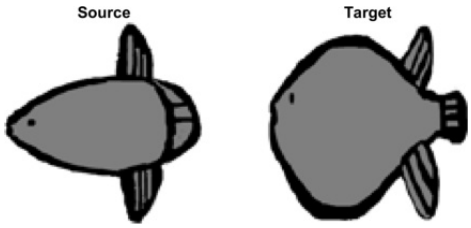

FIGURE 13. Swapped source and target images for Example 3.

To verify the robustness of our findings, we reverse the roles of the source and target images and choose a new set of labelled points, as demonstrated in Fig. 16. The resulting outcomes are displayed in Fig. 17. In this case, the image registration closely resembles the results shown in Fig. 15, which indicates that the process is not overly sensitive to the selection of the initial guess. This consistency across different configurations suggests that the registration process has likely reached a global minimum.

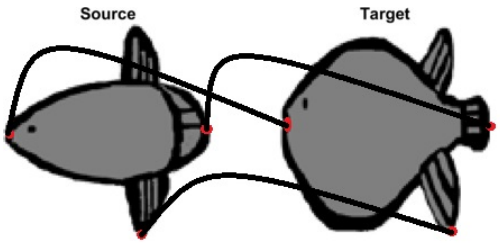

FIGURE 14. Corresponding labelled points are visible on the swapped pair—Example 3

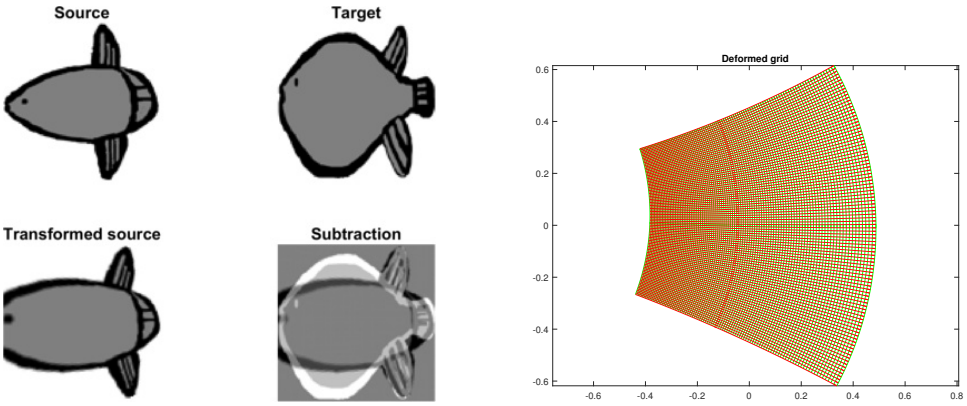

FIGURE 15. Results of Möbius registration, due to first set of landmarks, in Example 3 for the swapped dataset.

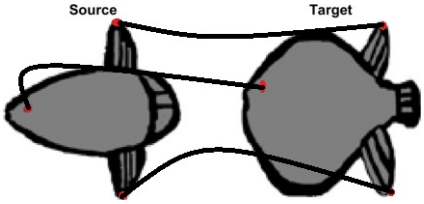

FIGURE 16. Selection of corresponding landmarks for Example 3: second set for second dataset.

3. CONCLUSION

In summary, this paper demonstrates that it is possible to effectively align or register images within a finite-dimensional group, with a particular focus on the Möbius group. The experimental results highlight that the selection of the initial condition plays a crucial role in determining the quality of the resulting registration, as well as influencing whether

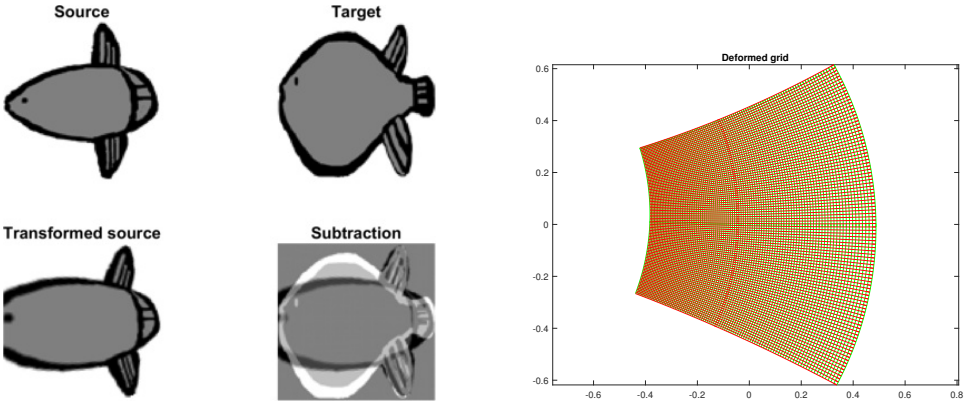

FIGURE 17. Möbius registration corresponding to the second choice of landmarks in a swapped dataset for Example 3.

the algorithm converges towards the neighborhood of the global minimum. While we cannot offer formal guarantees, the numerical experiments suggest that the algorithm has either reached the ultimate optimal solution or in the neighbourhood of it.

In the case of the image pair presented in Example 3, although definitive conclusions cannot be drawn, the results strongly imply that the registration process has been carried out within the Möbius group. However, the suboptimal registrations observed in certain instances indicate that the images in question may not be directly related by a Möbius transformation. These anomalies point to the need for further exploration and suggest that the registration of Thompson's fish images might require a more expansive group—one that encompasses the Möbius group as a subset. This suggests that a broader and more generalized framework could be necessary to fully capture the underlying transformation dynamics governing these images. Consequently, future research should focus on extending the registration process to a larger group in order to obtain more accurate, reliable, and insightful results.

4. FUNDING

There is no funding associated with this research.

5. CONFLICT OF INTEREST

The authors declare that they have no conflict of interest.

REFERENCES

[1] S. Aggarwal, *Principles of remote sensing*, Satellite Remote Sens. GIS Appl. Agric. Meteorol. **23**, No. 2 (2004) 23–28.

[2] J. Ali, M. K. Jamil, A. S. Alali, R. Ali, et al., *A medical image encryption scheme based on Möbius transformation and Galois field*, Heliyon **10**, No. 1 (2024).

[3] D. N. Arnold and J. P. Rogness, *Möbius transformations revealed*, Notices Amer. Math. Soc. **55**, No. 10 (2008) 1226–1231.

[4] M. F. Beg, M. I. Miller, A. Trouvé, and L. Younes, *Computing large deformation metric mappings via geodesic flows of diffeomorphisms*, Int. J. Comput. Vis. **61**, No. 2 (2005) 139–157.
[5] D. Bobalade, S. Joshi, and N. Sangle. *New subclass of analytic functions associated with fractional q¡ differintegral operator*, Punjab Univ. J. Math. **54**, No. 6 (2022) 347–359.
[6] F. L. Bookstein, *Foundations of morphometrics*, Annu. Rev. Ecol. Syst. **13**, No. 1 (1982) 451–470.
[7] F. L. Bookstein, *Morphometric tools for landmark data: geometry and biology*, Cambridge University Press, Cambridge, 1997.
[8] F. L. Bookstein, *The measurement of biological shape and shape change*, Springer Science & Business Media, New York, 2013.
[9] L. G. Brown, *A survey of image registration techniques*, ACM Comput. Surv. **24**, No. 4 (1992) 325–376.
[10] Y. Cao, M. I. Miller, R. L. Winslow, and L. Younes, *Large deformation diffeomorphic metric mapping of vector fields*, IEEE Trans. Med. Imaging **24**, No. 9 (2005) 1216–1230.
[11] L. Cattell, J. A. Schnabel, J. Declerck, and C. Hutton, *Combined PET–MR brain registration to discriminate between Alzheimer's disease and healthy controls*, in *Int. Workshop Biomed. Image Regist.*, 134–143, Springer, 2014.
[12] P. E. Clark and M. L. Rilee, *Remote sensing tools for exploration: observing and interpreting the electromagnetic spectrum*, Springer Science & Business Media, New York, 2010.
[13] I. Cohen and G. Medioni, *Detecting and tracking moving objects for video surveillance*, in *Proc. IEEE Comput. Soc. Conf. Comput. Vis. Pattern Recognit.*, Vol. 2 (1999) 319–325.
[14] I. L. Dryden and K. V. Mardia, *Statistical shape analysis: with applications in R*, John Wiley & Sons, Hoboken, 2016.
[15] L. M. G. Fonseca and M. H. M. Costa, *Automatic registration of satellite images*, in *Proc. X Brazilian Symp. Comput. Graph. Image Process.*, 219–226, IEEE, 1997.
[16] G. V. Gerganov, K. K. Mitev, and I. Kawrakow, *Iterative non-rigid image registration based on Möbius transformations*, in *Proc. IEEE Nucl. Sci. Symp. Conf. Rec.*, 2973–2975, IEEE, 2011.
[17] J. Glaunes, A. Qiu, M. I. Miller, and L. Younes, *Large deformation diffeomorphic metric curve mapping*, Int. J. Comput. Vis. **80**, No. 3 (2008) 317–336.
[18] J. Glaunès, M. Vaillant, and M. I. Miller, *Landmark matching via large deformation diffeomorphisms on the sphere*, J. Math. Imaging Vis. **20**, No. 1 (2004) 179–200.
[19] U. Grenander and M. I. Miller, *Computational anatomy: An emerging discipline*, Q. Appl. Math. **56**, No. 4 (1998) 617–694.
[20] Y. Gurefe, E. Mısırlı, et al. *Generalization of special functions and explicit form of fractional derivative of rational functions*, Punjab Univ. J. Math. **56**, No. 9 (2024) 525–542.
[21] E. Haber and J. Modersitzki, *Numerical methods for volume preserving image registration*, Inverse Probl. **20**, No. 5 (2004) 1621–1638.
[22] R. A. Heckemann, J. V. Hajnal, P. Aljabar, D. Rueckert, and A. Hammers, *Automatic anatomical brain MRI segmentation combining label propagation and decision fusion*, NeuroImage **33**, No. 1 (2006) 115–126.
[23] Y. Hu, M. Gong, Z. Qiu, J. Liu, H. Shen, M. Yuan, X. Zhang, H. Li, H. Lu, and J. Liu, *Coph100: A comprehensive fundus image registration dataset from infants constituting the "ridirp" database*, Sci. Data **12**, No. 1 (2025) 99.
[24] M. Jamil and X. Yang, *A literature survey of benchmark functions for global optimisation problems*, Int. J. Math. Modelling Numer. Optim. **4**, No. 2 (2013) 150–194.
[25] M. Jenkinson, P. Bannister, M. Brady, and S. Smith, *Improved optimization for the robust and accurate linear registration and motion correction of brain images*, NeuroImage **17**, No. 2 (2002) 825–841.
[26] M. Jenkinson and S. Smith, *A global optimisation method for robust affine registration of brain images*, Med. Image Anal. **5**, No. 2 (2001) 143–156.
[27] S. C. Joshi and M. I. Miller, *Landmark matching via large deformation diffeomorphisms*, IEEE Trans. Image Process. **9**, No. 8 (2000) 1357–1370.
[28] W. A. Kalender, S. Buchenau, P. Deak, M. Kellermeier, O. Langner, M. van Straten, S. Vollmar, and S. Wilharm, *Technical approaches to the optimisation of CT*, Phys. Med. **24**, No. 2 (2008) 71–79.
[29] S. L. Keeling and W. Ring, *Medical image registration and interpolation by optical flow with maximal rigidity*, J. Math. Imaging Vis. **23**, No. 1 (2005) 47–65.
[30] K. Knopp, *Elements of the Theory of Functions*, Dover Publications, New York, 1952.

[31] T. Liu, Z. Zhang, G. Fan, N. Li, C. Xu, B. Li, G. Zhao, and S. Zhou, *FocusMorph: A novel multi-scale fusion network for 3D brain MR image registration*, Pattern Recognit. (2025) 111761.
[32] L. F. Marcus, E. Bello, and A. García-Valdecasas, *Contributions to morphometrics*, Consejo Superior De Investigaciones Científicas, Spain, 1993.
[33] L. F. Marcus, M. Corti, A. Loy, G. J. P. Naylor, and D. E. Slice, *Advances in morphometrics*, Springer Science & Business Media, New York, 2013.
[34] MathWorks, *LSQNONLIN documentation*, available online (2022).
[35] J. Modersitzki and B. Fischer, *Optimal image registration with a guaranteed one-to-one point match*, in *Bildverarb. für die Medizin 2003*, 1–5, Springer, 2003.
[36] T. Needham, *Visual complex analysis*, Oxford University Press, New York, 1998.
[37] N. Nkanza, *Image registration and its application to computer vision: mosaicing and independent motion detection*, Master's thesis, University of Cape Town, 2005.
[38] A. T. Oladipo. *New subclasses of analytic univalent functions involving poisson distribution series bounded by generalized pascal snail*, Punjab Univ. J. Math. **56**, No. 2 (2024), 7–14.
[39] S. V. Petukhov, *Non-Euclidean geometries and algorithms of living bodies*, Comput. Math. Appl. **17**, 4–6 (1989) 505–534.
[40] J. Pieprzyk, H. Wang, and X. Zhang, *Möbius transforms, coincident boolean functions and non-coincidence property of boolean functions*, Int. J. Comput. Math. **88**, No. 7 (2011) 1398–1416.
[41] R. Rockne, E. C. Alvord, J. K. Rockhill, and K. R. Swanson, *A mathematical model for brain tumor response to radiation therapy*, J. Math. Biol. **58**, No. 4 (2009) 561–578.
[42] F. J. Rohlf and L. F. Marcus, *A revolution in morphometrics*, Trends Ecol. Evol. **8**, No. 4 (1993) 129–132.
[43] T. Sabisch, A. Ferguson, and H. Bolouri, *Automatic registration of complex images using a self organizing neural system*, in *1998 IEEE Int. Joint Conf. Neural Netw.*, Vol. 1, 165–170, IEEE, 1998.
[44] E. Saucan, E. Appleboim, E. Barak-Shimron, R. Lev, and Y. Y. Zeevi, *Local versus global in quasi-conformal mapping for medical imaging*, J. Math. Imaging Vis. **32**, No. 3 (2008) 293–311.
[45] G. Scholtz, D. Knötel, and D. Baum, *D'Arcy W. Thompson's cartesian transformations: a critical evaluation*, Zoomorphology **139**, No. 3 (2020) 293–308.
[46] C. G. Small, *The statistical theory of shape*, Springer Science & Business Media, New York, 2012.
[47] S. M. Smith, M. Jenkinson, M. W. Woolrich, C. F. Beckmann, T. E. J. Behrens, H. Johansen-Berg, P. R. Bannister, M. De Luca, I. Drobnjak, D. E. Flitney, et al., *Advances in functional and structural MR image analysis and implementation as FSL*, NeuroImage **23** (2004) S208–S219.
[48] D. W. Thompson, *On growth and form*, Cambridge University Press, New York, 1917.
[49] L. Tsang, K. Ding, S. Huang, and X. Xu, *Electromagnetic computation in scattering of electromagnetic waves by random rough surface and dense media in microwave remote sensing of land surfaces*, Proc. IEEE **101**, No. 2 (2012) 255–279.
[50] M. Y. Tufail and S. Gul, *Image registration using the rigid group*, Sci. Inq. Rev. **7**, No. 1 (2023) 71–86.
[51] M. Y. Tufail and S. Gul, *Conformal image registration using the discretized Cauchy–Riemann equations*, ANZIAM J. **67** (2025) e8.
[52] M. Y. Tufail and S. Gul, *Conformal patterns in the growth of human skulls*, Acta Biotheor. **73**, No. 3 (2025) 13.
[53] Y. Xiong, K. Zhu, D. Lin, and X. Tang, *Recognize complex events from static images by fusing deep channels*, in *Proc. IEEE Conf. Comput. Vis. Pattern Recognit.*, 1600–1609, 2015.
[54] L. Younes, *Shapes and diffeomorphisms*, Springer Science & Business Media, New York, 2010.